Polarization Properties of Semiconductor Nanorod Heterostructures: From Single Particles to the Ensemble

ARTICLE *in* JOURNAL OF PHYSICAL CHEMISTRY LETTERS · JANUARY 2013

Impact Factor: 7.46 · DOI: 10.1021/jz3021167

5 AUTHORS, INCLUDING:

Ido Hadar
Hebrew University of Jerusalem
10 PUBLICATIONS **124** CITATIONS
SEE PROFILE

Gal B Hitin
Hebrew University of Jerusalem
2 PUBLICATIONS **41** CITATIONS
SEE PROFILE

Amit Sitt
Columbia University
18 PUBLICATIONS **377** CITATIONS
SEE PROFILE

Adam Faust
Hebrew University of Jerusalem
17 PUBLICATIONS **213** CITATIONS
SEE PROFILE

THE JOURNAL OF PHYSICAL CHEMISTRY Letters

Letter

pubs.acs.org/JPCL

Polarization Properties of Semiconductor Nanorod Heterostructures: From Single Particles to the Ensemble

Ido Hadar, Gal B. Hitin, Amit Sitt, Adam Faust, and Uri Banin*

Institute of Chemistry and the Center for Nanoscience and Nanotechnology, The Hebrew University, Jerusalem 91904, Israel

Supporting Information

ABSTRACT: Semiconductor heterostructured seeded nanorods exhibit intense polarized emission, and the degree of polarization is determined by their morphology and dimensions. Combined optical and atomic force microscopy were utilized to directly correlate the emission polarization and the orientation of single seeded nanorods. For both the CdSe/CdS sphere-in-rod (S@R) and rod-in-rod (R@R), the emission was found to be polarized along the nanorod's main axis. Statistical analysis for hundreds of single nanorods shows higher degree of polarization, p, for R@R (p = 0.83), in comparison to S@R (p = 0.75). These results are in good agreement with the values inferred by ensemble photoselection anisotropy measurements in solution, establishing its validity for nanorod samples. On this basis, photoselection photoluminescence excitation anisotropy measurements were carried out providing unique information concerning the symmetry of higher excitonic transitions and allowing for a better distinction between the dielectric and the quantum-mechanical contributions to polarization in nanorods.

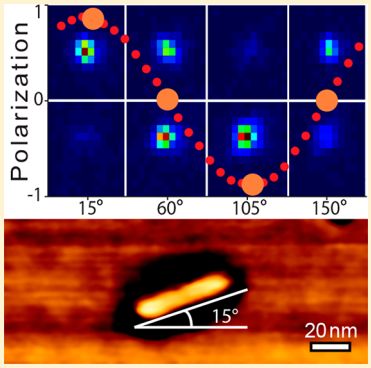

SECTION: Physical Processes in Nanomaterials and Nanostructures

Semiconductor nanocrystals (SC NCs) exhibit unique optical properties that can be tuned by modifying their composition, shape, and size.[1,2] Elongated NCs, also known as nanorods (NRs), show linearly polarized absorption and emission.[3−6] Given this significant advantage, a major drawback of NRs, in comparison to spherical NCs, is that their fluorescence quantum efficiency is typically lower. The reduced quantum efficiency is mainly due to the reduced spatial overlap between the electron and the hole wave functions that decreases the radiative decay rate, and also to the large surface area that increases the probability for surface trapping consequently increasing the nonradiative decay rate.[7] Indeed, growth of core/shell NRs has yielded so far only moderate values of fluorescence quantum yield for these systems compared to nanodots.[8,9] Seeded NR heterostructures constructed of a spherical seed embedded in an elongated rod-shaped shell (S@R) can overcome these limitations providing high quantum efficiencies along with linearly polarized emission.[10−12] Nevertheless, the degree of polarization in S@Rs is lower than that of single-component NRs as was shown both in single particle and ensemble measurements.[3,4,7,10,11] Seeded rod-in-rod (R@R) systems were recently introduced by us, as a new kind of heterostructured NCs constructed from an NR seed embedded within another rod, which show both high quantum efficiency and highly polarized emission.[13] These qualities arise from the combination of the properties of both the elongated seed together with a highly passivating shell, typical to the seeded growth approach. These attributes, as well as other spectroscopic properties and the robust synthesis that results in narrow size distributions, make these nanostructures favorable candidates for various optical and optoelectronic applications.[14−16] Additionally, as they bridge between the zero- (0D) to one-dimensional (1D) nanostructures, these heterostructures also serve as interesting model systems for the evolution of optical and electronic properties with dimensionality.

Here we report a single-particle study of the polarization characteristics of CdSe/CdS R@R and S@R, and in particular we present for the first time the direct correlation between the angle of emission polarization of a single NR to its physical orientation obtained using an atomic force microscope (AFM) scan. Utilizing the average degree of polarization obtained from the single-particle measurements, ensemble photoselection photoluminescence excitation (PS-PLE) anisotropy measurements were performed on both R@R and S@R systems. From these measurements, information regarding the symmetry of high excitonic transitions was extracted, showing the differences between the two systems, and leading to further understanding of their electronic structure.

S@R and R@R samples were synthesized following literature procedures.[11−13] Figure 1a,b presents the absorption and emission spectra of two samples, one R@R and the other S@R, together with their transmission electron microscopy (TEM) images. For both samples, the absorption at wavelengths above 500 nm is attributed to excitonic transitions mainly related to the CdSe core. The absorption band edge transition is more pronounced in the R@R sample due to the larger volume of the CdSe seed in this system. The significant

Received: December 19, 2012
Accepted: January 19, 2013
Published: January 19, 2013

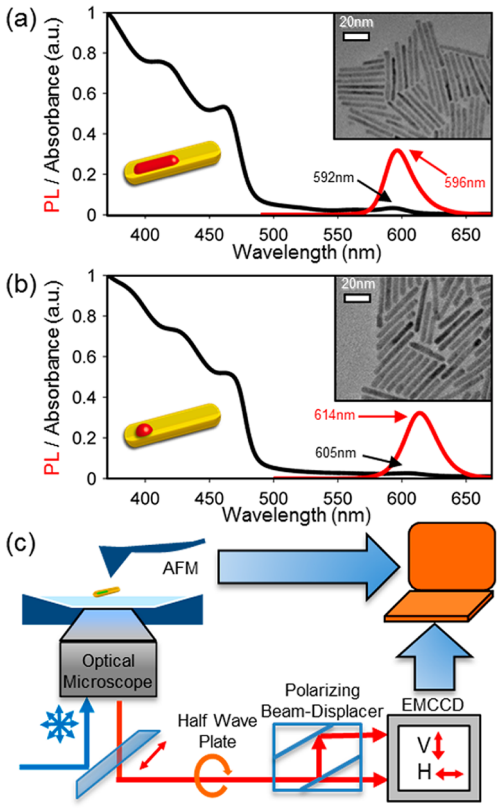

Figure 1. (a) Absorption and PL spectra for the R@R sample: 9 nm × 2.2 nm CdSe NR embedded in a 40 nm × 3.8 nm CdS rod shell. (b) Absorption and PL spectra for the S@R sample: 3.4 nm CdSe sphere embedded in a 45 nm × 5 nm CdS rod shell. Insets show TEM images and schematic diagrams of the particles. (c) The experimental setup for single particle measurements; see text for details.

increase in the absorption at wavelengths lower than 500 nm is attributed to the onset of absorption into the CdS rod transitions, and it is strongly pronounced because of the relatively large volume of the CdS shell. The emission in both systems is obtained from the band edge, which in these systems is well separated from the absorption edge of the CdS shell, as it arises from states with significant contribution of the CdSe seed. The emission from the S@R system is slightly red-shifted due to the larger diameter of the seed and the shell in this case. The relatively narrow emission spectra and the appearance of several well-defined peaks in the absorption spectra indicate narrow size distributions in both systems.

In order to obtain direct correlation between the emission polarization and spatial orientation of the NRs, an experimental setup, which includes an AFM mounted on top of an inverted optical microscope, was used, as depicted in Figure 1c. The combined setup enables one to measure the emission of single NRs and to determine the degree of polarization and polarization angle, and also to directly measure the NR's spatial orientation using the AFM. For single-particle measurements, a dilute solution of NCs in toluene was spin-coated onto a microscope cover glass such that the density of the particles was less than $1/\mu m^2$, typically resulting in 10−20 particles per frame. Fluorescence measurements were done in epi-illumination configuration. The NCs were excited using an unpolarized light-emitting diode (LED) at 470 ± 20 nm. The light emitted from the particles passes through a rotating half wave plate, which rotates the polarization vector of the emission. The emitted light then passes through a polarizing beam displacer, which separates the light into two orthogonal polarization components (horizontal and vertical) and shifts them spatially one with respect to the other. The image of the two polarizations is measured simultaneously using an electron multiplying charge coupled device (EMCCD) yielding significant improvement in the signal-to-noise ratio for the polarization determination. It should be noted that in the chosen measurement scheme, the emission polarization vector is rotated rather than the polarizer (as is often done[3,4]). While these two approaches are equivalent, fixing the polarizer with respect to the measurement system reduces unwanted effects related to different response of the measurement system to the different polarizations.

Optical measurements were conducted on several hundreds of single NRs from each sample, and their degree of polarization and polarization angle were calculated. AFM measurements were performed on several tens of single NRs. One of the complications of single particle measurements, and consequently their interpretation, is blinking, wherein the emission intensity of the single particle drops down rapidly and then recovers.[17] However, as the calculation of the polarization factor effectively normalizes the measurement to the overall intensity, measuring both polarization components simultaneously allows overcoming these fluctuations in the intensity. Thus, under the presented measurement scheme, the blinking does not affect the polarization measurements, and useful data can be obtained even from measurements in which the particle emission underwent blinking (see Supporting Information S1).

Figure 2a shows subsequent fluorescence images of a single R@R particle at the two orthogonal polarizations measured simultaneously at different rotation angles of the half wave plate. The linear polarization characteristic is clearly seen from the systematic intensity variations in the two orthogonal polarizations. The intensity of both polarization components is extracted from the different images, and the polarization factor for each angle is calculated according to $P = (I_H - I_V)/(I_H + I_V)$, where I_H (I_V) is the intensity of the horizontal (vertical) polarization component. These values are well fitted by a sinusoidal function, which yields the polarization angle and the degree of polarization for each NR. This is shown in Figure 2b for the same particle presented in 2a (blue line) and for two other representative particles (green and red lines). The phase shifts between the curves indicate the different polarization angle of each single NR.

Thereafter, an AFM scan of the same region was acquired. Correlation of the AFM data with the optical image with submicrometer resolution is realized, allowing imaging of the same NRs measured optically (see Supporting Information S2). This was applied to directly determine the spatial orientation of the rod, allowing us to correlate it with the emission polarization angle. Figure 2c−e shows AFM phase images of the same NRs shown in Figure 2b (red, blue, and green curves, respectively). The elongated rod shape is evident, allowing determination of the orientation angle, while the rods appear slightly wider due to the convolution effect of the tip. The orientation for the rods was measured to be 5°, 125°, and 135° (±5°), in excellent agreement with the PL polarization angles of the same rods: 7°, 124°, and 133° (±1°), respectively. While the good correspondence of the polarization and rod orientation is to be expected, to the best of our knowledge this is the first direct correlation of this property for single NRs.

dx.doi.org/10.1021/jz3021167 | J. Phys. Chem. Lett. 2013, 4, 502−507

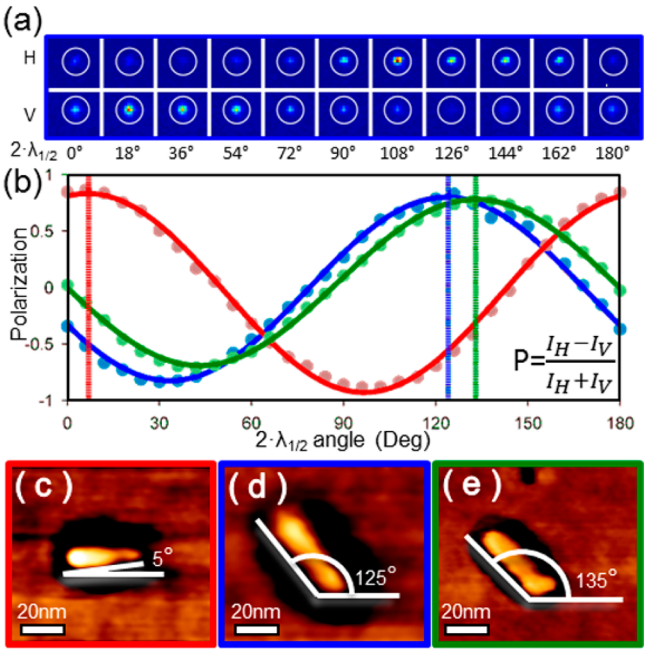

Figure 2. Correlated optical polarization and AFM measurements of single NRs. (a) Fluorescence images of a single R@R taken at wave plate angles from 0° to 90°. Two orthogonal polarizations (*H*,*V*) were recorded simultaneously clearly showing the polarized emission from the single rods. (b) Emission polarization factor ($P = (I_H - I_V)/(I_H + I_V)$), calculated from the images above (blue solid circles) and fitted to a sinusoidal function (blue solid line) to give a polarization factor of 0.81 at 124°. Red (R@R) and green (S@R) curves show similar curves for additional particles measured by the same method to give polarization factors of 0.88 and 0.74 at alignment angles of 7° and 133°, respectively. (c,d,e) AFM phase images of the NRs, represented by the red, blue, and green curves, showing physical orientation of 5°, 125°, and 135°, respectively, all in good agreement with the emission polarization (scale bar 20 nm).

Figure 3 shows the histogram of measured polarization values for R@R (Figure 3a) and S@R (Figure 3b) particles, from which mean emission polarization values were extracted. For the R@R sample, the mean polarization value is $p_{(R@R)}$ = 0.83

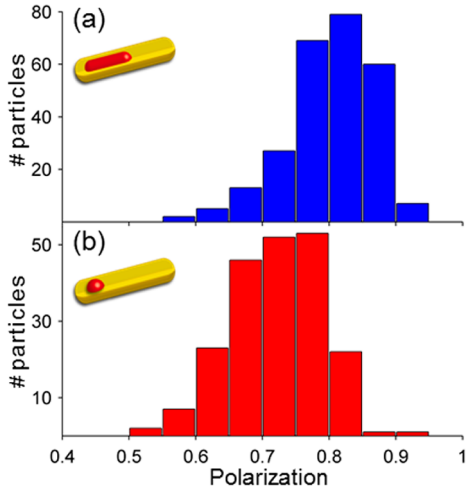

Figure 3. Histograms of polarization values obtained from (a) 262 single R@Rs with an average polarization value of 0.83 (STD = 0.06) and (b) 207 single S@Rs with an average polarization value of 0.75 (STD = 0.07).

with relatively narrow distribution (STD of 0.06), showing good agreement with values previously obtained for single-component NRs in single-particle measurements (experimentally: 0.86,[3] and theoretically: 0.87[18,19]). For the S@R sample, the mean polarization is lower, $p_{(S@R)}$ = 0.75, and also similar to values measured previously for single seeded rods (0.75[10]). This sample shows a slightly broader distribution (STD of 0.07) but nevertheless is still relatively uniform. Similar analysis for another S@R sample with broader size distribution shows almost the same average polarization (0.74), but exhibited a broader distribution of polarization values (see Supporting Information S3). This demonstrates the powerful feature of the single-particle study, directly providing the distribution.

The difference in polarization values of the R@R and S@R structures arises because the emission originates primarily from the seed. Considering R@R, even without the CdS rod-shell, the CdSe rod seed itself is expected to yield linearly polarized emission along the rod's axis. The growth of the shell further reinforces the polarization while enhancing the quantum yield. In the case of S@R, however, the spherical cores are known to exhibit 2D plane polarization.[20−22] Consequently, the build-up of the linear polarization is directly related to the growth of the CdS rod-shell, and is mediated by the crystal field effect and the cylindrical symmetry exerted by the shell.[13]

Single-particle polarization measurements provide a better distinction between emission and absorption polarization in a direct way, which is not possible in ensemble photoselection measurements.[23,24] Yet, the single particle experiments require much more effort. Recently we demonstrated how the band edge photo selection measurements can be used to extract the emission polarization value.[13] This analysis assumed that the band edge absorption transition is completely polarized (P_{abs} = 1). This assumption is based on contributions both from electronic transitions polarized along the rod's axis, a quantum mechanical effect, as well as from a classical dielectric effect, affected by the composition and the rod's aspect-ratio, which reduces the electric field perpendicular to the rod axis, causing induced absorption parallel to the rod's axis.[25] It has also been suggested that as the excitation shifts more to the blue, the electronic polarization contribution in absorption decreases due to overlapping states, until eventually the absorption degree of polarization is attributed almost completely to the dielectric effect.

The single particle experiments allow us now to directly verify the above-mentioned assumptions that were used to calculate the emission polarization from the band edge anisotropy. To this end, PS-PLE measurements were carried out on the R@R and S@R samples in solution. In this method, a solution of NCs in toluene is excited using vertically polarized light, and the PLE spectrum is measured separately for each emission component : parallel (vertical) and perpendicular (horizontal). From these spectra, the anisotropy factor can be calculated for each excitation wavelength according to $r = (I_{\parallel} - I_{\perp})/(I_{\parallel} + 2I_{\perp})$. Due to the random orientation of the NRs in the solution, the anisotropy values may vary between r = 0.4 for the case of an excitation dipole moment parallel to the emission dipole moment, and r = −0.2 for the case of excitation dipole moment perpendicular to the emission dipole moment.[23,24]

For the R@R sample, the measured band edge anisotropy value was $r_{R@R}$ = 0.29. Using the emission degree of polarization, $p_{emission}$ = 0.83, obtained from the single particle measurements, the sample absorption degree of polarization

dx.doi.org/10.1021/jz3021167 | J. Phys. Chem. Lett. 2013, 4, 502−507

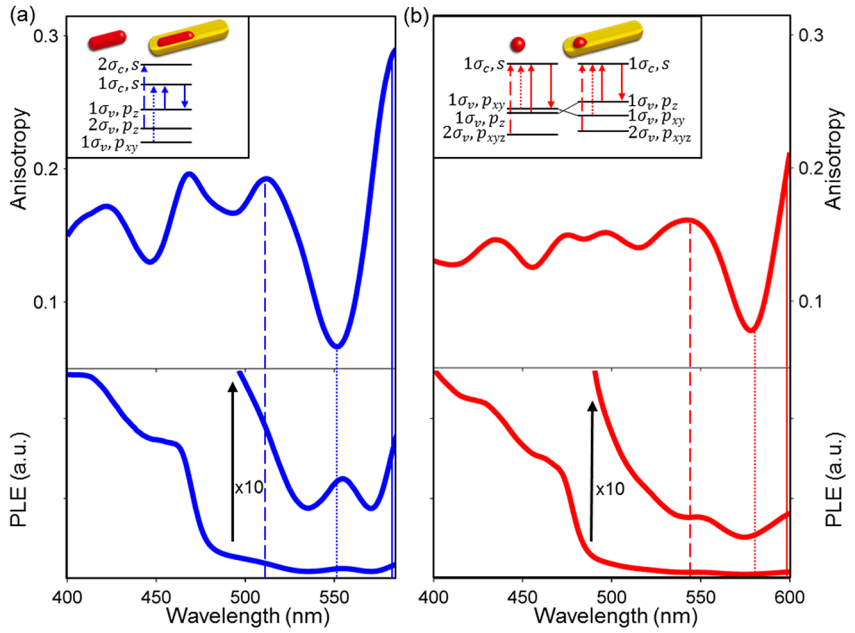

Figure 4. PLE scan—photo selection anisotropy factor (top frames) and photoluminescence intensity (lower frames), as a function of excitation wavelength for (a) R@R and (b) S@R dissolved in toluene. Extrema in the anisotropy scan match features in the PLE scan, but are significantly more pronounced. Vertical lines indicate assigned excited state absorption transitions, solid lines indicate the band edge transition, and dotted and dashed lines indicate the second and third transitions, respectively. Inset in the upper panel shows a schematic energy diagram of the assigned transitions (not to scale). Inset in the lower panel shows ×10 magnification of the PLE scan near the band edge.

can now be directly extracted and is $p_{abs} = 0.97$ (see Supporting Information S4). As for the S@R, the measured band edge anisotropy is $r_{S@R} = 0.22$, the degree of emission polarization from the single-particle study is $p_{emission} = 0.75$, yielding a band edge absorption degree of polarization of $p_{abs} = 0.88$. For both samples, there is similar contribution of the dielectric effect to the polarization factor due to the similar dimensions of the CdS rod-shell. However, the electronic contribution is different between the two structures since the fundamental transition arises from the seed. For the sample with a rod shaped seed, the first transition is strongly polarized, while for the spherical seed the linearly polarized transition becomes favorable only upon the growth of the shell, and it is not as strongly polarized. Consequently, for the R@R sample, the band edge absorption polarization factor is very close to the assumed value of 1, whereas for the S@R sample the value is slightly lower, yet still much higher than the contribution of the dielectric effect alone. These results demonstrate the validity of using the band edge anisotropy measured in the ensemble, as a tool to calculate the single NR emission polarization as discussed above.

Additionally, PS-PLE measurements also reveal spectroscopic information regarding the NRs electronic structure. Figure 4a,b show the PLE and the corresponding PS-PLE spectra for R@R and S@R, excited at wavelengths ranging from 400 nm to the NRs band edge. The spectra exhibit various minima and maxima of anisotropy, most of which correspond to electronic absorption transitions of the respective particles. The features observed in the anisotropy scan generally match those observed in the PLE spectrum, but they are much more pronounced, demonstrating how PS-PLE better resolves optical transitions. At short wavelengths, below 400 nm, there is almost no electronic contribution to the absorption polarization, and the anisotropy reaches an asymptotic value of $r \approx 0.15$, which arises from the dielectric effect alone.[13]

For the longer wavelengths (energy below the shell band edge), the PLE intensity drops down rapidly, since the absorbance in this regime is only to the seed transitions, which has significantly reduced oscillator strength due to the small seed volume compared to the rod shell. Anisotropy in general, and PS-PLE in particular, does not depend on the total intensity but rather on the ratio between the two orthogonal polarization components, thus providing convenient and powerful means to measure simultaneously both shell and seed transitions. Additionally, for the anisotropy spectrum, allowed transitions appear both as maxima or minima according to their symmetry, while in PLE spectra they only appear as maxima of the emission intensity; this was recently also reported for colloidal semiconductor nanoplate.[26] Apart from the additional data regarding the symmetry of the transitions, variation between the minimum and maximum values can also help to distinguish between close transitions that are not easily discerned in the PLE due to broadening, thus offering an improvement of the experimental resolution.

The effects of shell growth on the electronic structure can be inferred from comparison of the optical transitions observed in the PS-PLE spectra for the CdSe seed, which is of wurtzite structure (below the CdS band edge energy), to transitions previously reported for CdSe nanodots and NRs.[27−29] For the R@R sample, the second and third transitions in PS-PLE spectrum are shifted by 150 and 300 meV from the band edge respectively; both match values obtained experimentally for CdSe NRs with similar energy gap.[27] The assignment of the transitions is done based on published pseudopotential calculations for short NRs with an aspect ratio of 3.1.[19,29] For these NRs as well as for spherical NCs, the states are classified using the notation $(n\sigma_{c/v}, l_m)$, where n represents the quantum number of the envelope function along the z-direction, either in the valence (σ_v) or conduction (σ_c) band, and l_m represents the predominant atomic orbitals associated with the state. The

dx.doi.org/10.1021/jz3021167 | J. Phys. Chem. Lett. 2013, 4, 502−507

band edge transition and the third transition seen as maxima in the PS-PLE spectrum, match the $(1\sigma_v, p_z) \rightarrow (1\sigma_c, s)$ and $(2\sigma_v, p_z) \rightarrow (2\sigma_c, s)$ transitions, respectively, which originate mainly from *z*-polarized states and thus are polarized along the rod long axis. The second transition, seen as a minimum in PS-PLE, is assigned to the $(1\sigma_v, p_{xy}) \rightarrow (1\sigma_c, s)$ transition that is polarized perpendicular to the rod long axis (*xy*-planar polarized state). These results match by symmetry recent absorption transitions measurements of CdSe nanowires,[30] as expected since the polarization originates from the atomic orbital nature of the states, while the quantization along the *z*-direction, which is lost for long NR or nanowires, affects their energies but not the polarization.

For the S@R it is already well established that the emission polarization becomes linear, and here we also observe that the excited state absorption spectrum is substantially different from the one obtained for spherical CdSe NCs (aspect ratio of 1), mainly in the symmetry of the transitions. For spherical NC, the band edge transition is composed of two close transitions: the first one plane-polarized $(1\sigma_v, p_{xy}) \rightarrow (1\sigma_c, s)$ and the second *z*-polarized $(1\sigma_v, p_z) \rightarrow (1\sigma_c, s)$.[19,29] This should yield *xy*-plane polarization as shown for nearly spherical NCs.[20−22] By contrast, our measurement for S@R clearly shows that the band edge transition is *z*-polarized and the second transition is *xy*-polarized. The seed electronic level structure has undergone a fundamental change upon shell growth also for the excited states, and for the heterostructure the *z*-polarized transition becomes lower in energy and is separated from the *xy*-polarized transition. The crossing of the levels originates mainly from the strong crystal field effect mediated by the CdS rod shell, lowering the energy of the *z*-polarized transition.[31] For both samples additional transitions appear at energies above the CdS shell band edge energy dominated primarily by the CdS levels.

In conclusion, the emission polarization of single R@R heterostructures was measured quantitatively, and its value was found to conform with the ensemble NRs' degree of polarization measured by photoselection. For S@R, a lower degree of emission polarization was reaffirmed. The straightforward correlation between the NR's emission polarization and the spatial orientation determined by AFM was revealed directly for single NR heterostructures. The single particle study has provided validation for extracting the emission polarization from ensemble band edge anisotropy values. The use of PS-PLE anisotropy measurements as a tool to explore the electronic transitions was demonstrated, and this technique bears substantial advantages over ordinary PLE measurements, providing a detailed view of the emission and absorption characteristics of anisotropic semiconductor rod heterostructures.

EXPERIMENTAL METHODS

Synthesis of NRs. Heterostructured CdSe@CdS R@R and S@R systems were synthesized by the seeded growth approach.[11−13] In this method the seed and shell growth are done in two separate steps. First, CdSe rods or dots are grown to serve as seeds. These seeds are then cleaned from excess ligands by repetitive precipitation in toluene/methanol mixture. For the second step, the seeds are mixed with elemental sulfur and dissolved in trioctyl phosphine (TOP), the mixture is swiftly injected into a flask containing trioctyl phosphine oxide (TOPO), hexyl phosphonic acid (HPA), octadecyl phosphonic acid (ODPA), and CdO and heated to 360 °C under Ar atmosphere. The reaction is kept at this temperature for a few minutes, and afterward the flask is allowed to cool to room temperature.

Single-Particle Measurements. The experimental setup for single-particle polarization measurements is based on an AFM (JPK NanoWizard 3) mounted on top of an inverted optical microscope (Nikon Eclipse Ti). Illumination of the sample is done using a white unpolarized LED (Prizmatix) in Epi-illumination configuration, focused through a high numerical aperture (N.A.) oil immersion objective (X100 1.4 N.A., Nikon). The fluorescence is collected through the same objective and filtered spectrally, and then passes a rotating half wave plate, a polarizing beam displacement prism, and is collected by an EMCCD (Andor iXon3). In a typical measurement, the wave plate (and thus the particle polarization angle) is rotated in steps of 3°, and a fluorescence image is recorded for each angle. In these images each single particle appears as two equidistant spots, each represents either horizontal or vertical polarization. These images are processed by a home-written Matlab code that automatically matches pairs of spots correspond to a single particle, integrates the intensity for each polarization component, calculates the polarization at each angle, and fits the data to a sinusoidal function. The degree of polarization and angle for each NR are extracted from the fit.

Ensemble PS-PLE Anisotropy Measurements. For ensemble anisotropy experiments, a solution of nanoparticles in toluene is prepared and its absorption is measured, verifying the maximum optical density of 0.1. The sample is measured in an L-shaped spectrometer (Edinburgh instruments F920). During measurement, the sample is illuminated with vertically polarized light at a range of wavelengths (400 nm to band edge) by a monochromatized super continuum laser (Fiannium). Vertical and horizontal fluorescence components are measured subsequently. After normalization for the different detection efficiencies of each polarization component, anisotropy is calculated for each wavelength.

ASSOCIATED CONTENT

Supporting Information

Additional information regarding processing of the optical data, correlation between AFM and optical measurements, additional sample studied, and calculation of absorption degree of polarization. This material is available free of charge via the Internet at http://pubs.acs.org

AUTHOR INFORMATION

Corresponding Author

*E-mail address: banin@chem.ch.huji.ac.il.

Notes

The authors declare no competing financial interest.

ACKNOWLEDGMENTS

The research leading to these results has received funding from the European Research Council under the European Union's Seventh Framework Programme (FP7/2007−2013)/ERC Grant Agreement No. 246841. U.B. thanks the Alfred & Erica Larisch memorial chair.

REFERENCES

(1) Alivisatos, A. P. Semiconductor Clusters, Nanocrystals, and Quantum Dots. *Science* **1996**, *271*, 933−937.

(2) Murray, C. B.; Norris, D. J.; Bawendi, M. G. Synthesis and Characterization of Nearly Monodisperse CdE (E = Sulfur, Selenium,

Tellurium) Semiconductor Nanocrystallites. *J. Am. Chem. Soc.* **1993**, *115*, 8706−8715.
(3) Hu, J.; Li, Ls; Yang, W.; Manna, L.; Wang, Lw; Alivisatos, A. P. Linearly Polarized Emission from Colloidal Semiconductor Quantum Rods. *Science* **2001**, *292*, 2060−2063.
(4) Chen, X.; Nazzal, A.; Goorskey, D.; Xiao, M.; Peng, Z.; Peng, X. Polarization Spectroscopy of Single CdSe Quantum Rods. *Phys. Rev. B* **2001**, *64*, 2−5.
(5) Rothenberg, E.; Ebenstein, Y.; Kazes, M.; Banin, U. Two-Photon Fluorescence Microscopy of Single Semiconductor Quantum Rods: Direct Observation of Highly Polarized Nonlinear Absorption Dipole. *J. Phys. Chem. B* **2004**, *108*, 2797−2800.
(6) Krahne, R.; Morello, G.; Figuerola, A.; George, C.; Deka, S.; Manna, L. Physical Properties of Elongated Inorganic Nanoparticles. *Phys. Rep.* **2011**, *501*, 75−221.
(7) Peng, X.; Manna, L.; Yang, W.; Wickham, J.; Scher, E.; Kadavanich, A.; Alivisatos, A. P. Shape Control of CdSe Nanocrystals. *Nature* **2000**, *404*, 59−61.
(8) Manna, L.; Scher, E. C.; Li, L.-S.; Alivisatos, A. P. Epitaxial Growth and Photochemical Annealing of Graded CdS/ZnS Shells on Colloidal CdSe Nanorods. *J. Am. Chem. Soc.* **2002**, *124*, 7136−7145.
(9) Mokari, T.; Banin, U. Synthesis and Properties of CdSe/ZnS Core/Shell Nanorods. *Chem. Mater.* **2003**, *15*, 3955−3960.
(10) Talapin, D. D. V.; Koeppe, R.; Götzinger, S.; Kornowski, A.; Lupton, J. M.; Rogach, A. L.; Benson, O.; Feldmann, J.; Weller, H. Highly Emissive Colloidal CdSe/CdS Heterostructures of Mixed Dimensionality. *Nano Lett.* **2003**, *3*, 1677−1681.
(11) Carbone, L.; Nobile, C.; De Giorgi, M.; Della Sala, F.; Morello, G.; Pompa, P.; Hytch, M.; Snoeck, E.; Fiore, A.; Franchini, I. R.; et al. Synthesis and Micrometer-Scale Assembly of Colloidal CdSe/CdS Nanorods Prepared by a Seeded Growth Approach. *Nano Lett.* **2007**, *7*, 2942−2950.
(12) Talapin, D. V; Nelson, J. H.; Shevchenko, E. V; Aloni, S.; Sadtler, B.; Alivisatos, A. P. Seeded Growth of Highly Luminescent CdSe/CdS Nanoheterostructures with Rod and Tetrapod Morphologies. *Nano Lett.* **2007**, *7*, 2951−2959.
(13) Sitt, A.; Salant, A.; Menagen, G.; Banin, U. Highly Emissive Nano Rod-in-Rod Heterostructures with Strong Linear Polarization. *Nano Lett.* **2011**, *11*, 2054−2060.
(14) Deka, S.; Quarta, A.; Lupo, M. G.; Falqui, A.; Boninelli, S.; Giannini, C.; Morello, G.; De Giorgi, M.; Lanzani, G.; Spinella, C.; et al. CdSe/CdS/ZnS Double Shell Nanorods with High Photoluminescence Efficiency and Their Exploitation as Biolabeling Probes. *J. Am. Chem. Soc.* **2009**, *131*, 2948−2958.
(15) Kazes, M.; Lewis, D. Y.; Ebenstein, Y.; Mokari, T.; Banin, U. Lasing from Semiconductor Quantum Rods in a Cylindrical Microcavity. *Adv. Mater.* **2002**, *14*, 317−321.
(16) Pisanello, F.; Martiradonna, L.; Spinicelli, P.; Fiore, A.; Hermier, J. P.; Manna, L.; Cingolani, R.; Giacobino, E.; De Vittorio, M.; Bramati, A. Dots in Rods as Polarized Single Photon Sources. *Superlattices Microstruct.* **2010**, *47*, 165−169.
(17) Nirmal, M.; Brus, L. Luminescence Photophysics in Semiconductor Nanocrystals. *Acc. Chem. Res.* **1999**, *32*, 407−414.
(18) Shabaev, A.; Efros, A. L. 1D Exciton Spectroscopy of Semiconductor Nanorods. *Nano Lett.* **2004**, *4*, 1821−1825.
(19) Hu, J.; Li, L.; Yang, W.; Alivisatos, A. P. Semiempirical Pseudopotential Calculation of Electronic States of CdSe Quantum Rods. *J. Phys. Chem. B* **2002**, *106*, 2447−2452.
(20) Empedocles, S. A.; Neuhauser, R.; Bawendi, M. G. Three-Dimensional Orientation Measurements of Symmetric Single Chromophores Using Polarization Microscopy. *Nature* **1999**, *399*, 126−130.
(21) Koberling, F.; Kolb, U.; Philipp, G.; Potapova, I.; Basché, T.; Mews, A. Fluorescence Anisotropy and Crystal Structure of Individual Semiconductor Nanocrystals. *J. Phys. Chem. B* **2003**, *107*, 7463−7471.
(22) Chung, I.; Shimizu, K. T.; Bawendi, M. G. Room Temperature Measurements of the 3D Orientation of Single CdSe Quantum Dots Using Polarization Microscopy. *Proc. Natl. Acad. Sci. U.S.A.* **2003**, *100*, 405−408.
(23) Kliger, D. S.; Lewis, J. W.; Einterz, R. C. *Polarized Light in Optics and Spectroscopy*, 1st ed.; Academic Press Inc.: San Diego, CA, 1990.
(24) Lakowicz, J. R. *Principles of Fluorescence Spectroscopy*, 3rd ed.; Springer: Singapore, 2006.
(25) Wang, J.; Gudiksen, M. S.; Duan, X.; Cui, Y.; Lieber, C. M. Highly Polarized Photoluminescence and Photodetection from Single Indium Phosphide Nanowires. *Science* **2001**, *293*, 1455−1457.
(26) Cassette, E.; Mahler, B.; Guigner, J.-M.; Patriarche, G.; Dubertret, B.; Pons, T. Colloidal CdSe/CdS Dot-in-Plate Nanocrystals with 2D-Polarized Emission. *ACS Nano* **2012**, *6*, 6741−6750.
(27) Katz, D.; Wizansky, T.; Millo, O.; Rothenberg, E.; Mokari, T.; Banin, U. Size-dependent Tunneling and Optical Spectroscopy of CdSe Quantum Rods. *Phys. Rev. Lett.* **2002**, *89*, 086801.
(28) Norris, D.; Bawendi, M. Measurement and Assignment of the Size-Dependent Optical Spectrum in CdSe Quantum Dots. *Phys. Rev. B* **1996**, *53*, 16338−16346.
(29) Li, J.; Wang, L.-W. High Energy Excitations in CdSe Quantum Rods. *Nano Lett.* **2003**, *3*, 101−105.
(30) McDonald, M. P.; Vietmeyer, F.; Kuno, M. Direct Measurement of Single CdSe Nanowire Extinction Polarization Anisotropies. *J. Phys. Chem. Lett.* **2012**, *3*, 2215−2220.
(31) Luo, Y.; Wang, L.-W. Electronic Structures of the CdSe/CdS Core-shell Nanorods. *ACS Nano* **2010**, *4*, 91−98.